A novel global multi-level terrain data tile production method

Zhen Wang[1], Wei Huang[1], Chang Gao[2,3], Cong Wang[1], Wenhao Zhao[1], Dejin Tang[1], Xinyan Zheng[1], Heng Li[1], Lei Ding[1], Zhengchang Han[4], Hongping Zhang[1]

[1] National Geomatics Center of China, Beijing, China- (wangzhen, huangwei, wangcong, zhaowenhao, tangdejin, zhengxinyan, liheng, dinglei, zhanghongping)@ngcc.cn

[2] BGP INC., China National Petroleum Corporation, Hebei, China- (gaochang03@cnpc.com.cn)

[3] Kunlun Digital Technology Co., Ltd. Beijing, China- (gaochang03@cnpc.com.cn)

[4] ShanDong ZhengYuan Geophysical Information Technology co.,LTD, Shandong, China - (sdzyhzc@126.com)

Keywords: Global, Terrain-RGB, Multi-level, Tiles, Terrain services.

Abstract

Terrain services have increasingly wide applications in urban planning, 3D gaming animation, and other fields. Map websites typically provide terrain services to users in the form of terrain shaded relief tiles. Map tile technology offers a new solution for large-scale concurrent user access. Although terrain shaded relief tiles can effectively represent changes in terrain relief, users cannot adjust the visualized raster images for visualization schemes, making data analysis and applications more challenging. The emergence of Terrain-RGB technology has effectively addressed this limitation. However, currently, internet maps mostly provide multi-level map services to users in the form of web map tile service (WMTS). Terrain-RGB images produced by simple encoding tools may exhibit grid lines when rendered on tiles with a small grid spacing, affecting the usability of Terrain-RGB products. Therefore, this paper proposes a technical approach for producing global multi-level Terrain-RGB products using digital elevation model (DEM), focusing on addressing the issues of gridlines and splicing traces from different scenes DEM data, offering a new solution for map websites to release analyzable terrain services.

1. Introduction

With the advancement of the social economy, geographic information data has garnered growing interest. Governments and commercial enterprises are increasingly offering geographic information services to users via map websites. Apart from delivering vector data (e.g., roads, buildings, green spaces) and imagery data (e.g., satellite imagery, aerial imagery) as standard layers, several platforms also provide terrain data and land cover classification data. For instance, the National GeoInformation Service Platform "Tianditu" (Zhang et al., 2021; Wang et al., 2022) is one such platform.

Terrain data plays a crucial role across various domains (Yu et al., 2020). In the context of terrain representation, terrain data serves to depict elevation information of the Earth's surface, facilitating users in comprehending the terrain and geomorphological characteristics of the land surface. By utilizing terrain data, users can acquire information pertaining to terrain attributes like ground elevation, mountains, rivers, valleys, and other geographical features. In the field of cartography, the elevation data conveyed by terrain data aids cartographers in accurately illustrating terrain characteristics like contour lines, terrain shading, and slope, consequently enhancing the realism and detail of map data. Within the realm of terrain analysis (Xiong et al., 2021), terrain data finds applications in diverse analyses such as terrain profile analysis, flood simulation, and visibility analysis. Through the analysis of terrain data, users can gain a better understanding of terrain features and make corresponding decisions and plans.

Map websites commonly deliver map services to users through map tile technology, which was pioneered by Google in 2005 with the introduction of Google Maps. Map tile technology partitions maps into numerous small pieces (tiles), with each tile representing a section of the map, stored and transmitted as image files. This approach facilitates users in browsing maps by dynamically loading tiles, thereby achieving rapid map loading and interactive experiences. Map tile technology serves as the cornerstone for the evolution of modern web maps and finds extensive application in other map services and geographic information systems (Guo et al., 2023; Wu et al., 2013). By preprocessing data through clipping and rendering it into tiles, map tile technology effectively addresses the challenge of simultaneous access by a large user base. Notably, the advent of new vector tile technology (Netek et al., 2020) organizes vector data into tiles, allowing for frontend rendering style modifications and enabling functionalities such as attribute queries and data analysis. However, once terrain data is converted into raster tiles, it becomes viewable and visualizable but loses its original elevation information, rendering it unsuitable for further analysis and processing.

The emergence of Terrain-RGB tiles has introduced new avenues for the analysis and processing of terrain-based tiles. Terrain-RGB employs a color-coding technique for map creation and visualization, integrating digital elevation model (DEM) data with a specific color-coding method to represent elevation information of the Earth's surface (Iwao et al., 2020). The elevation range of DEM data is mapped to a range within the RGB color space; for instance, low-altitude areas are depicted in blue, mid-altitude areas in green, and high-altitude areas in brown. This approach enables differentiation of various elevation areas on the map through distinct colors. The primary advantage of Terrain-RGB lies in the ability to decode the RGB colors of the image to retrieve the original elevation information of the DEM with an accuracy of 0.1 meters. Decoding the tiles to extract elevation information facilitates diverse visualization schemes and analytical applications, such as terrain slope calculation, hill shading display, and 3D terrain mesh generation for video or games.

Unlike the concept of scale in traditional maps, current internet maps offer users various levels of map services (typically ranging from level 1 to 18 or 20) through map tile technology. Calculated with each tile size of 256, the pixel size of level 18 tiles is 0.59 meters, while the pixel size of level 12 tiles is 38.2 meters. Common publicly available DEM/DSM products, such as ETOPO, GTOPO30, SRTM, GMTED2010, ASTER GDEM, AW3D30, and TanDEM-X DEM, have pixel sizes of 30 meters, 90 meters, or even worse. When utilizing these data to generate tiles with small grid spacing and subsequently rendering them, grid lines may appear internally, thereby impacting the usability of Terrain-RGB products. Moreover, there is currently no publicly available technical method for generating global multi-level Terrain-RGB tiles.

With the continuous advancement of Internet mapping technologies, there is a growing demand for analyses based on these maps. Terrain-RGB tiles offer a valuable means for performing terrain analyses, including slope analysis, aspect analysis, viewshed analysis, watershed analysis, and shadow analysis. Consequently, there is a pressing need for a technical method to generate global multi-level Terrain-RGB tiles.

The study utilizes 30-meter pixel size ASTER GDEM data to design a novel global multi-level terrain data tile production method, addressing the issues of grid lines appearing during rendering on tiles with a small grid spacing and the noticeable seam artifacts introduced at the boundaries of two images when stitching DEM data of different extents after pixel size changes. The structure of this paper is as follows. Section 2 provides detailed information about the dataset used in the study. Section 3 outlines the method for producing global multi-level Terrain-RGB tiles. Section 4 presents the tile results produced based on the technical approach designed in this paper. Finally, Section 5 summarizes the conclusions of this study.

2. Data

Various digital elevation product datasets have been publicly released internationally, with differences in data sources, spatial resolution, and coverage (Tang et al., 2021). The first global digital elevation product was ETOPO5, released in 1988, which was generated by integrating data from multiple countries. Most of the elevation data were obtained through traditional leveling or triangulation methods, resulting in inconsistent data sources, accuracy, and quality. The launch of the ASTER GDEM mission marked the beginning of satellite-based global digital elevation product production. Currently, satellite-based elevation measurements primarily include optical stereophotogrammetry, radar altimetry, and lidar altimetry, with ASTER GDEM being a type of data product obtained from optical stereophotogrammetry for global elevation. The ASTER instrument was launched in December 1999 aboard NASA's Terra spacecraft, featuring high spatial, spectral, and radiometric resolution, with the ability to acquire stereo data along its orbit in the near-infrared spectral band (Abrams et al., 2002).

ASTER GDEM offers data coverage for all terrestrial areas between 83°S and 83°N, boasting a resolution of 1 arc-second. The horizontal reference surface of ASTER GDEM is based on the WGS84 coordinate system, and the vertical reference surface is based on the EGM96 geoid (Varga and Bašić, 2013). ASTER GDEM v1 data products were released by NASA and METI, utilizing approximately 1.26 million optical stereo images. While these products were generated via fully automated processes, they suffered from issues such as cloud contamination, limited coverage in high-latitude regions, and certain artifacts (Hirt et al., 2010; Nikolakopoulos et al., 2006). After additional data supplementation (approximately 260,000 images), NASA and METI released ASTER GDEM v2, which showed significant improvements in coverage compared to v1. Building upon ASTER GDEM v2, ASTER GDEM v3 incorporated approximately 360,000 optical stereo image pairs to enhance spatial coverage and accuracy of elevation data (Fujisada et al., 2011; Fujisada et al., 2012). Furthermore, various algorithms were employed to mitigate anomalous data, thereby reducing blank areas in elevation values and improving overall data quality. This iterative refinement process led to significant enhancements in both coverage and accuracy of the dataset.

Each ASTER GDEM v3 data file contains a Digital Elevation Model (DEM) file recording elevation information and a NUM file recording quality assessment information. Each image data covers a real area of 1 degree by 1 degree, with the filename indicating the geometric center latitude and longitude of the pixel in the lower left corner of the covered area. Each image has dimensions of 3601 rows by 3601 columns. The adjacent two scenes of DEM data overlap by one row at the north-south edges or one column at the east-west edges, and the overlapping parts have the same values for the two scenes of data. Specific information about the data is provided in Table 1:

Tile Size	3601 x 3601 (1 degree by 1 degree)
resolution	1 arc-second (30 m)
Geographic coordinates	WGS84
DEM output format	DEM: GeoTiff, signed 16 bits, and 1m/DN for DEM; NUM: GeoTiff; unsigned 8 bit number of individual scenes used to compile each pixel (maxed at 50); and source of fill for missing ASTER data (see index below)
Special DN values	-9999 for void pixels and 0 for sea-level water body
Coverage	North 83 degrees to south 83 degrees, 22,912 tiles for GDEM

Table 1. The data characteristics of ASTER GDEM (Abrams et al., 2022)

3. Method

Figure 1 depicts the comprehensive procedure of the global multi-level terrain data tile production method, encompassing six main stages: mosaicking a single DEM data with the surrounding 8 DEM data, converting DEM data types, filling null values and conducting projection transformation, resampling and filtering DEM data, clipping DEM data, mosaicking DEM data of the same column, and encoding DEM elevation data into RGB format.

https://doi.org/10.5194/isprs-annals-X-3-2024-423-2024

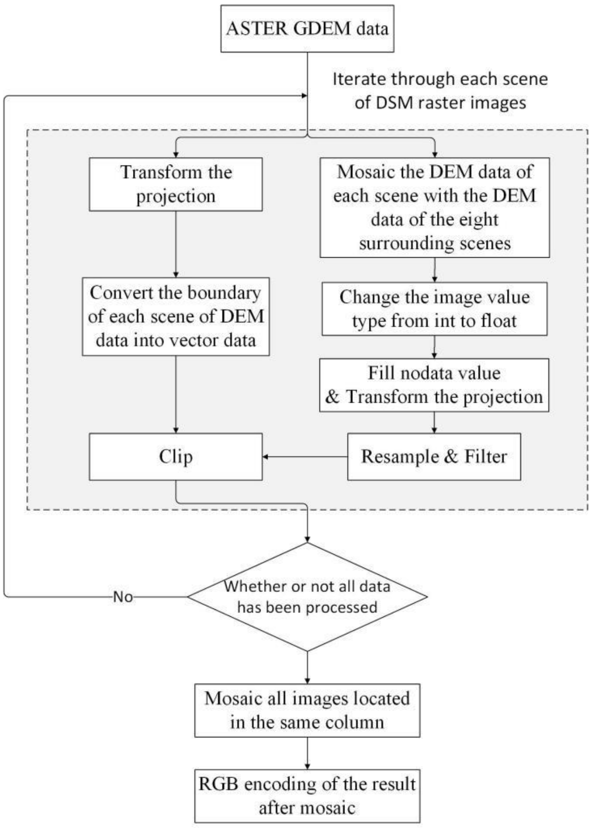

Figure 1. Operational flow about global multi-level terrain data tile production method.

3.1 Mosaic the DEM Data

Each scene of DEM data is represented as a 3601*3601 two-dimensional matrix. During the processing of matrix edge values, such as DEM reprojection and resampling, adjustments to the edge pixel values necessitate involving adjacent scenes of DEM data. As illustrated in Figure 2, the pixel 'a' from the DEM data in scene A will influence computations involving pixel 'b' from scene B; conversely, pixel 'b' from the DEM data in scene B will affect computations involving pixel 'a' from scene A. Consequently, it is imperative to mosaic the individual scenes of DEM data for processing.

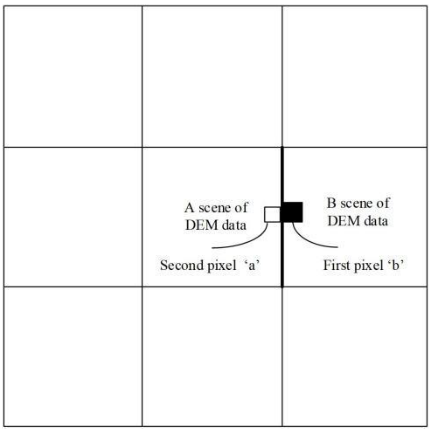

Figure 2. Schematic diagram of mosaic operation.

(1) For instance, when encoding a single scene of DEM data located at north latitude 30-31 degrees and west longitude 110-111 degrees (referred to as N30E110), all adjacent scenes of DEM data are retrieved. These include N29E109, N30E109, N31E109, N29E110, N31E110, N29E111, N30E111, and N31E111, totaling 8 scenes of DEM data.

(2) Due to the incomplete coverage of DEM data globally, missing data may occur when querying, particularly in oceanic areas. To ensure the automation of the processing workflow, missing DEM data is supplemented by generating a new scene of DEM data at the respective location based on parameters such as latitude and longitude range, spatial reference, and resolution. In the predominantly oceanic areas, elevation values are set to zero. This supplementation of DEM data is solely intended to automate the program, and the assignment of zero elevation values minimally affects only a few pixels at the boundaries.

(3) The GDAL Warp tool is utilized to mosaic the DEM data of N30E110 and its surrounding 8 scenes.

3.2 Change the DEM Data Value and Transform the Projection

(1) The elevation data within DEM datasets is typically stored as integer values. In order to enhance computational accuracy, it is imperative to convert the numerical representation of DEM data from integer (int) to floating point (float) prior to any computational processes.

(2) In order to address potential voids or missing data points within the original DEM dataset that cannot be encoded, the GDAL tool is employed to fill these nodata positions.

(3) Given that internet maps commonly utilize EPSG:3857 as the projection coordinate system, it becomes necessary to transform the DEM data to conform to this specific projection coordinate. During the transformation process, which involves recalculating the height values of the DEM, bilinear interpolation is utilized to ensure a balance between computational accuracy and efficiency.

3.3 Resample and Filter the DEM Data

(1) Different DEM products have varying pixel sizes, typically ranging from 90 meters, 30 meters, to 10 meters. Internet maps offer map services at multiple levels through WMTS, with each level having a different pixel size. For instance, level 11 corresponds to 76.437028 meters, level 12 to 38.218514 meters, level 13 to 19.109257 meters, and level 14 to 9.554629 meters. Consequently, when generating data for different levels, the original DEM data must undergo resampling to match the pixel size of each level. For example, to generate map tile data spanning levels 1 to 13, the original DEM data must be resampled to 19.109257 meters. To ensure data consistency and prevent discontinuities or internal gridlines, cubic convolution is employed for resampling. As shown in Figure 3, for the sake of illustration, we demonstrate the resampling process using only the DEM data from the middle scene after mosaic (though in reality, the resampling process applies to the entire DEM data after mosaic). The 3*3 grid is resampled to a 4*4 grid (the number of grid cells shown here is for illustrative purposes only and does not represent the actual number of grid cells). The value of each pixel within the 4*4 grid needs to be calculated based on the values of the surrounding 16 pixels.

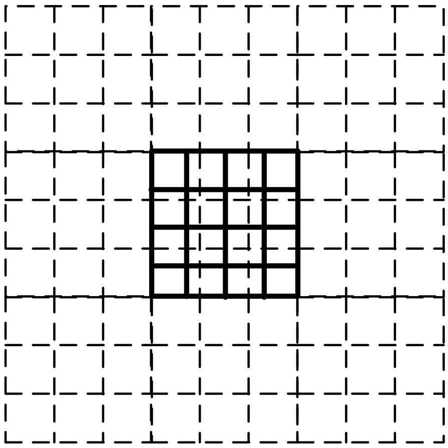

Figure 3. Schematic diagram of resampling.

(2) The original DEM data may include noise points, outliers, and other irregularities. To minimize the influence of these anomalies and prevent discontinuities or internal gridlines, the resampled data undergo mean filtering. A filter window size of 9*9 is employed for this filtering process.

3.4 DEM Data Clipping

Firstly, we projected the original DEM data to EPSG3857. Then, we converted the boundaries of the projected DEM data into vector data. Finally, we clipped the filtered mosaic DEM data using the boundary vector data.

Processing the DEM data of the central scene involved incorporating data from the surrounding eight scenes. This approach not only enhances the accuracy of calculations but also resolves the issue of different values at overlapping boundaries caused by resampling operations.

3.5 Mosaic All DEM Data Located in the Same Column

To enhance encoding efficiency and minimize the number of files for encoding, DEM data within the same column are merged and mosaicked.

3.6 RGB Encoding of the Result After Mosaic

The elevation information of the filtered DEM is encoded, with each original elevation value being represented by three values: red (R), green (G), and blue (B).

In this encoding approach, the decoding algorithm operates as follows:

$$\text{value} = \text{int}\big((\text{height} + 10000) * 10\big) \quad (1)$$

$$\text{R} = (\text{value} \gg 16) \quad (2)$$

$$\text{G} = (\text{value} \gg 8 \,\&\, 255) \quad (3)$$

$$\text{B} = (\text{value} \,\&\, 255) \quad (4)$$

Where height represents the elevation value of DEM data, ">>" denotes the right shift operator, and "&" denotes the bitwise AND operator.

The specific calculation process involves the following steps: Firstly, calculate the "value" based on the elevation value of DEM data. Next, convert the decimal value of "value" to binary. Then, shift the binary value of "value" right by 16 bits to obtain the R value. Subsequently, shift the result obtained by shifting the binary value of "value" right by 8 bits and perform a bitwise AND operation with binary value 255 to obtain the G value. Finally, perform a bitwise AND operation with binary value 255 on the binary value of "value" to obtain the B value. By utilizing the RGB channels collectively to represent the elevation height of each pixel, the resulting Terrain-RGB map can provide a more intuitive display of the elevation value of each pixel.

Terrain-RGB employs the three 8-bit integer channels of an RGB file format to collectively represent the elevation height, allowing for 16,777,216 unique values mapped to an elevation increment of 0.1 meters. This ensures the vertical accuracy required for mapping purposes. The following formula (1) can be used to recalculate the elevation value:

$$\text{Height} = -10000 + \big((\text{R} * 256 * 256 + \text{G} * 256 + \text{B}) * 0.1\big) \quad (5)$$

4. Results and Discussion

We conducted experiments following the designated procedure to generate Terrain-RGB terrain data using ASTER GDEM v3. The experiments primarily aimed to address two issues, as depicted in Figure 4: firstly, the occurrence of internal grid lines when rendering on tiles with a small grid spacing; secondly, the noticeable seam artifacts at the boundaries of two images when the data is processed only by resampling. The presence of gridlines is attributed to the rendering level necessitating a DEM resolution higher than that of the original DEM data. The seam artifacts arise from resampling, causing discrepancies in the values of overlapping columns or rows between two DEM datasets.

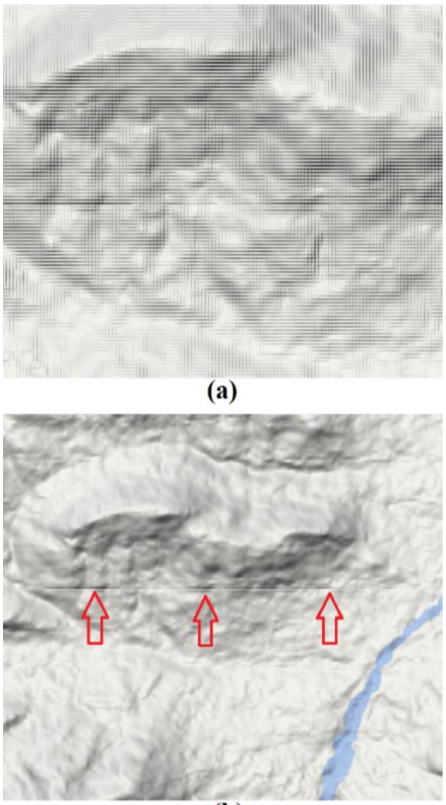

(a)

(b)

Figure 4. (a) The grid lines; (b) The seam artifacts at the boundaries of two images (the red arrow points to the seam).

4.1 The Results of Generating Novel Tiles

As illustrated in Figure 5, we presented the outcomes post-mosaicking. The red-bordered triangles are located at the four corners of the middle scene DEM. From Figure 5, it is evident that owing to the overlapping rows and columns in adjacent positions of each scene's DEM data, no discernible seams are visible in the mosaic of the original DEM data. The darker color of the DEM in the middle scene is due to the expansion of the DEM value range after mosaicking, and the two DEMs show differences by stretching the value range. Despite the capability to render the single-band DEM in color, once released into tiles, extracting the original elevation information from the images becomes unfeasible.

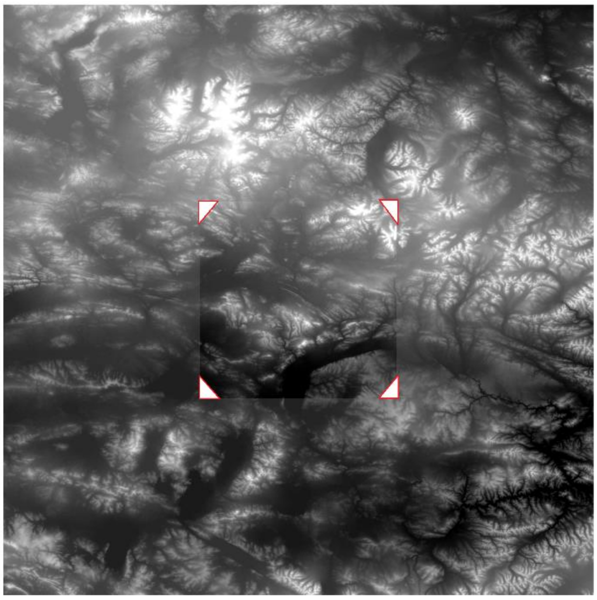

Figure 5. The results after mosaicking.

Following the procedures outlined in Chapter 3 Method, we conducted sequential operations including reprojection, resampling, and filtering on the mosaic data. Subsequently, we clipped the DEM data corresponding to the middle scene from the mosaic result. Then, we mosaicked the data from the same column. Finally, the combined data from the entire column was encoded into RGB.

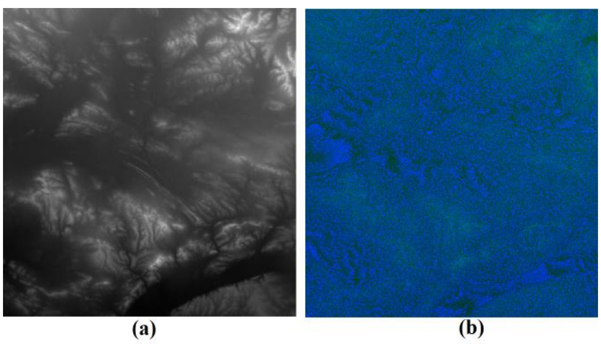

Figure 6. (a) Original DEM data; (b) Data after RGB encoding.

From Figure 6, it is evident that the original single-band DEM data has been transformed into three-band RGB data through encoding. Crucially, even after the RGB-encoded data is tiled, elevation information can still be extracted by reading the R, G, and B values of the images.

We conducted a comparison between directly encoding DEM data into RGB and the method proposed in this paper. Both sets of results were rendered with hillshade shading and then zoomed in to level 13. As depicted in Figure 7, the gridline issue has been effectively resolved using the method proposed in this paper.

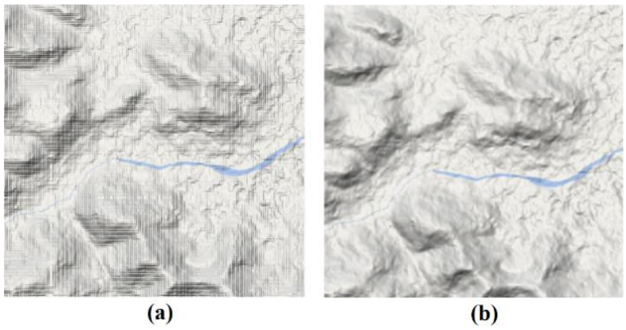

Figure 7. (a) Rendering result of the original DEM after RGB encoding; (b) Rendering result after RGB encoding using the method proposed in this paper.

4.2 The Application of Novel Tiles

Additionally, we conducted tests to explore some advantages of Terrain-RGB. These include directly retrieving elevation in the frontend using tiles and modifying rendering styles directly in the frontend. Furthermore, various terrain analyses, such as flood analysis, visibility analysis, and slope aspect analysis, can be performed using this technique.

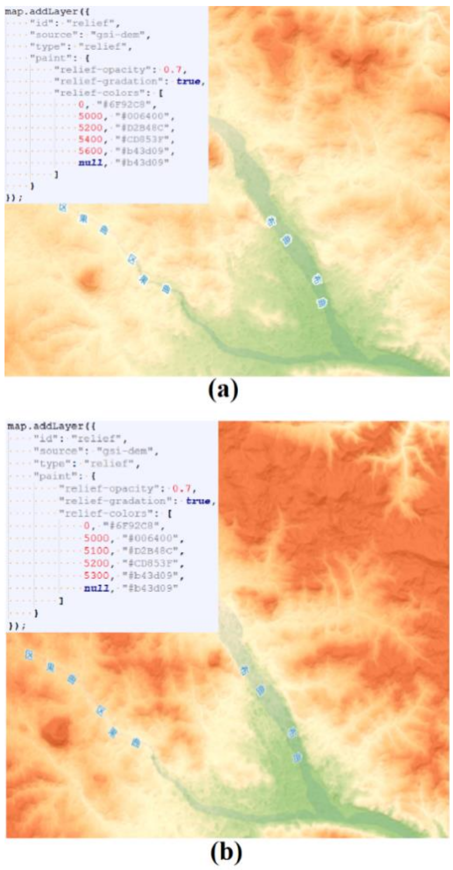

Figure 8. Using frontend code to directly modify the rendering style of map tiles. The frontend rendering code is located in the upper left corner. Map tile area is the Qinghai-Tibet Plateau region.

As depicted in Figure 8, we have the capability to directly define colors for display based on elevation values. We used the JavaScript library provided by Maobox (Mapbox GL JS), which is widely used to build web maps and web applications. In the code snippet provided in the top left corner, the "relief-opacity" parameter is utilized to adjust the transparency of the rendering result, while "relief-gradation" determines whether the rendering should be layered. Lastly, the "relief-colors" parameter is employed to render the tiles according to elevation using specified colors. Figure 9 illustrates that we can acquire elevation information of the terrain surface by directly clicking on the tiles in the frontend. We obtain the RGB value of the tile click position and combine it with formula (5) to get the elevation of the click position.

Figure 9. Click on the tile to retrieve elevation information for the clicked location.

We employed the method in this paper to generate global terrain tiles, which were subsequently rendered with hillshade. The rendering outcomes were superimposed onto global land and ocean surfaces, as depicted in Figure 10. These results underscore the effectiveness of the proposed approach, which can be implemented in websites offering global map services. Additionally, by replacing data sources, data ranges, and method parameters, it is also possible to produce new terrain tiles of various levels for specific target areas.

Figure 10. The global tiles produced using the method described in this paper.

5. Conclusion

The demand for various terrain analyses based on Internet terrain maps is increasing. However, significant challenges remain in generating global multi-level Terrain-RGB tiles using existing DEM products. This paper presents a novel technique for producing global multi-level terrain data tiles. The main steps of the method include: Initially, we mosaic individual DEM data with surrounding DEM data from eight scenes. Subsequently, the mosaic DEM data undergoes various operations including type conversion, null value filling, and projection transformation. Following this, the transformed DEM data is resampled and filtered. Finally, through steps such as DEM data clipping, concatenation of DEM data from the same column, and RGB encoding of DEM elevation data, global multi-level terrain tile data is generated.

The innovative terrain tiles enable the inference of surface elevation information through the combination of the R, G, and B channels. With this technology, we can query and analyze the terrain tiles, thereby significantly expanding the range of terrain tile applications.

In future research, we aim to leverage the novel terrain tiles for representing three-dimensional scenes and explore their application capabilities in various scenarios such as games, virtual reality, and overlaying optical image data.

Acknowledgements

We would like to express our gratitude to Mapbox for sharing their innovative tile encoding algorithm. Additionally, we extend our appreciation to the ASTER GDEM v3 generation team for sharing the DEM data.

References

Abrams, M., Hook, S., Ramachandran, B. 2002. ASTER user handbook, version 2. Jet propulsion laboratory, 4800, 135.

Abrams, M., Yamaguchi, Y., Crippen, R. 2022. Aster Global Dem (GDEM) Version 3. The International Archives of the Photogrammetry, Remote Sensing and Spatial Information Sciences, 43, 593-598.

Fujisada, H., Urai, M., Iwasaki, A. 2011. Advanced methodology for ASTER DEM generation. IEEE transactions on geoscience and remote sensing, 49(12), 5080-5091.

Fujisada, H., Urai, M., Iwasaki, A. 2012. Technical methodology for ASTER global DEM. IEEE Transactions on Geoscience and Remote Sensing, 50(10), 3725-3736.

Guo, M., Wu, L., Huang, Y., Chen, X. 2023. An efficient internet map tiles rendering approach on high resolution devices. Journal of Spatial Science, 68(1), 3-21.

Hirt, C., Filmer, M. S., Featherstone, W. E. 2010. Comparison and validation of the recent freely available ASTER-GDEM ver1, SRTM ver4. 1 and GEODATA DEM-9S ver3 digital elevation models over Australia. Australian Journal of Earth Sciences, 57(3), 337-347.

Iwao, K., Nishioka, Y., Kitao, K. 2020. Web-Based Sea Level Change Simulation System Using PNG Elevation Tiles and Smart Tile Architecture. Journal of Geographic Information System, 12(4), 291-301.

Netek, R., Masopust, J., Pavlicek, F., Pechanec, V. 2020. Performance testing on vector vs. raster map tiles—comparative study on load metrics. ISPRS International Journal of Geo-Information, 9(2), 101.

Nikolakopoulos, K. G., Kamaratakis, E. K., Chrysoulakis, N. 2006. SRTM vs ASTER elevation products. Comparison for two regions in Crete, Greece. International Journal of remote sensing, 27(21), 4819-4838.

Tang X.，Li S.，Li T.，Gao Y.，Zhang S.，Chen Q. Zhang X. 2021. Review on global digital elevation products. National Remote Sensing Bulletin，25（1）：167-181

Varga, M., Bašić, T. 2013. Quality assessment and comparison of global digital elevation models on the territory of Republic of Croatia. Kartografija i geoinformacije, 12(20), 4-17.

Wang, Z., Huang, W., Zhang, H., Wang, C., Tang, D., Zheng, X., Ding, L. 2022. Location Discovery of Vector Data Update Driven by Map Image Tiles for National Geo-Information Service Platform. The International Archives of the Photogrammetry, Remote Sensing and Spatial Information Sciences, 43, 211-216.

Wu, H., Guan, X., Liu, T., You, L., Li, Z. 2013. A high-concurrency web map tile service built with open-source software. Modern accelerator technologies for geographic information science, 183-195.

Xiong, L., Tang, G., Yang, X., Li, F. 2021. Geomorphology-oriented digital terrain analysis: Progress and perspectives. Journal of Geographical Sciences, 31, 456-476.

Yu, X., Lu, D., Jiang, X., Li, G., Chen, Y., Li, D., Chen, E. 2020. Examining the roles of spectral, spatial, and topographic features in improving land-cover and forest classifications in a subtropical region. Remote Sensing, 12(18), 2907.

Zhang, H., Huang, W., Jiang, J., Du, M., Yang, J. 2021. A High-Currency Geo-Spatial Service Gateway for National GeoInformation Service Platform. The International Archives of Photogrammetry, Remote Sensing and Spatial Information Sciences, 43, 383-388.